Journal of Applied Geology, vol. 8(1), 2023, pp. 34–47
DOI: http://dx.doi.org/10.22146/jag.60835

Identification of permeable structures and heat source in the geothermal working area of Galunggung Volcano and the heat source connectivity to the Karaha-Cakrabuana Area using gravity data

Leo Agung Prabowo[1], Salahuddin Husein[*2], and Sismanto[3]

[1]*PT Fairbanc Technologies Indonesia. Gedung South Quarter Tower A, Lt. 18, Unit D-G Cilandak Barat, Jakarta Selatan*
[2]*Department of Geological Engineering, Faculty of Engineering, Universitas Gadjah Mada, Yogyakarta, Indonesia*
[3]*Geophysics SubDepartment, Department of Physics, Faculty of Mathematics and Science, Gadjah Mada University Yogyakarta, Indonesia*

Received: October 25, 2020 | Accepted: May 5, 2023 | Published online: August 20, 2023

ABSTRACT. Galunggung volcano is a geothermal concession area adjacent to the Karaha-Cakrabuana concession area with a distance of around 1 km. The Indonesian Government plans to build a power plant in 2025, so additional research is needed to support the plan. A gravity survey could help identify permeable structures (fault) and heat sources to a certain depth. The data processing results showed faults seen on the FHD, SVD, and ABL residual maps, while heat sources were shown from the closed contour patterns on the ABL, residual, and regional maps. Derivative analysis strengthens the position and type of fault from the match between the maximum FHD value and zero SVD value. These results identified the existence of three faults in the study area, and were all identified as normal faults. 3D modeling gave a picture of density contrast in the research area. From the section profile that passes through Galunggung and Telaga Bodas craters, the heat source was interpreted as density with value 2.8–3.0 gr/cm^3 and marked by orange to red color that coincides below Galunggung crater and continued to Talaga Bodas crater at depths below -3000 masl. This indicates that both concession areas were connected.

Keywords: Galunggung · Gravity method · Derivative analysis · 3D model.

1 INTRODUCTION

Galunggung Volcano is one of the volcanos located in West Java and adjacent to the Karaha-Cakrabuana concession area with the potential for geothermal energy. Galunggung concession area was located west of Tasikmalaya (Figure 1). Galunggung Volcano itself has 264 Mwe geothermal energy potential. Previous studies have suggested that the Galunggung volcano has sufficient geothermal energy and needs better studies (Ramadhan et al., 2016; Fadillah et al., 2013).

In 2025, Kementerian Energi dan Sumberdaya Mineral RI (2017), Indonesia Government planned to build a power plant in the Galunggung concession area. With 264 Mwe geothermal energy potential and the plan 2025 to build a power plant, various surveys, including gravity surveys, were needed to support it. A gravity survey was needed because it can differentiate gravitation fields in various places, leading to density (Lowrie, 2007). The author used a gravity survey to identify the geothermal area's geological structures and heat sources. To identify geological structures, the derivative analysis method was used to provide a better under-

*Corresponding author: S. HUSEIN, Department of Geological Engineering, Universitas Gadjah Mada. Jl. Grafika 2 Yogyakarta, Indonesia. E-mail: shddin@ugm.ac.id

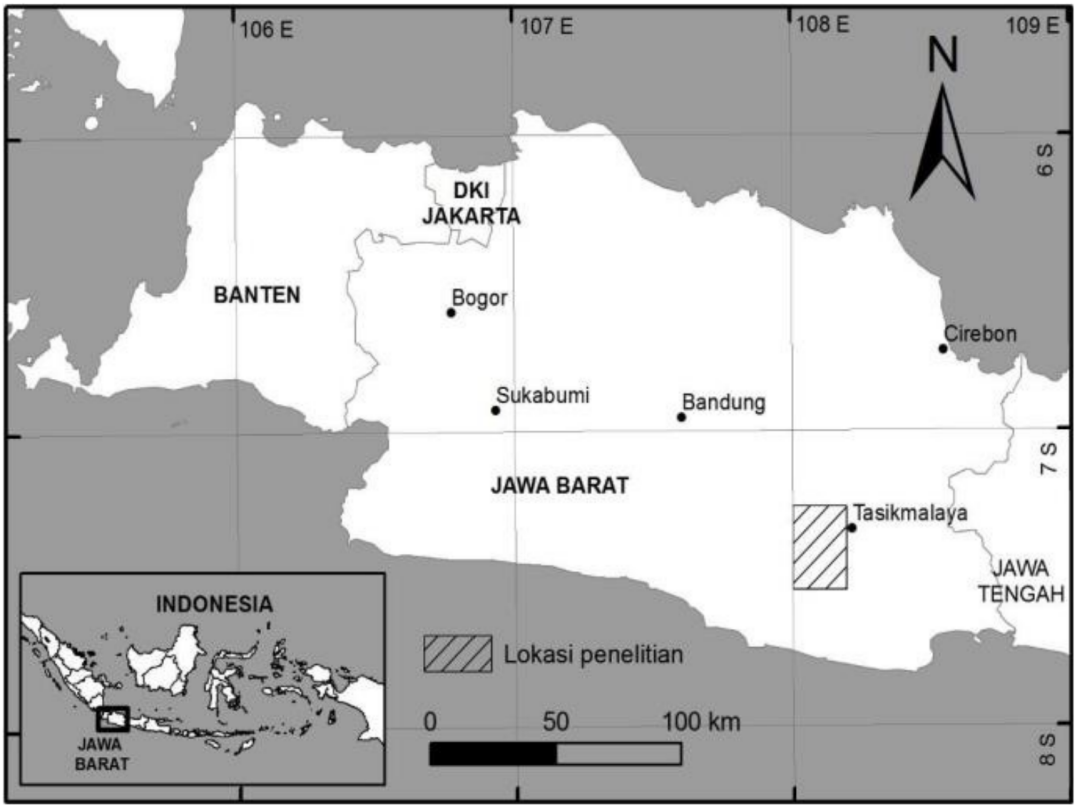

FIGURE 1. Location of Galunggung concession area.

standing and to identify heat sources, 3D modeling was used to provide a better illustration.

Gravity data used for processing was obtained from satellite gravity data GGMplus. Curtin University, Australia, provided the satellite data. The satellite data resolution was 7.2 arc-second or close to ~200-meter resolution spatially (Hirt et al., 2013).

2 GEOLOGY OF GALUNGGUNG VOLCANO

Physiographically, the Galunggung volcano is located in the Quaternary Volcanoes zone and adjacent to the Bandung zone (depressed zone in the middle of Java island) in the north and Southern Mountains in the south (Van Bemmelen, 1949). Geology structures formation in Galunggung concession area affected by tectonism in Java Island. The tectonic plate that played an active role was the Eurasian plate and the Indian-Australian plate (Hall, 2002). The tectonism resulted in 3 dominant patterns in Java. The patterns were Meratus, Sundanese, and Javanese (Pulunggono and Martodjojo, 1994). Locally, the geological structure in the Galunggung concession area was dominated by normal faults, as seen from the Geology Map of Tasikmalaya (Budhitrisna, 1990). The identification of normal faults near the Galunggung crater was supported by fumarole in the crater's center (Bronto, 1989). The other geological structures (normal faults) needed to be proven, so the gravity survey was conducted to try to answer these.

In the Galunggung concession area, there were 3 dominant lithology units as seen in the Geology Map of Tasikmalaya (Budhitrisna, 1990). The 3 units were Galunggung Breccia, Old Volcano Product (such as volcanic breccia, tuff, and lava), and Young Volcano Product (such as volcanic breccia and tuff). There were also diorite intrusion, andesite intrusion, and dacite intrusion. The geology map of the Galunggung area in the geology map of the Tasikmalaya Sheet from Figure 2.

3 METHODS

The gravity method is a method to measure and map the variety of subsurface gravity acceleration laterally (Jacoby & Smilde, 2009). In exploration, gravity acceleration is usually called gravity. The variety that affects gravity value is rock density. Rock density is defined as the

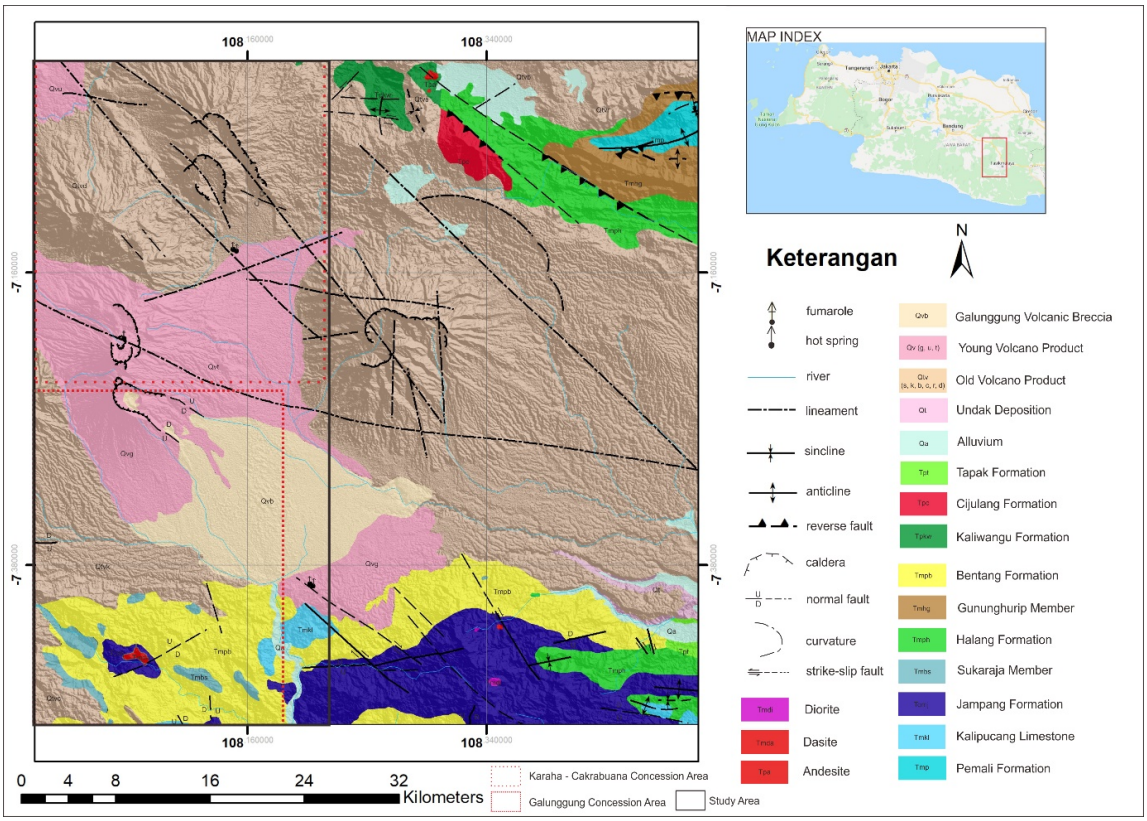

FIGURE 2. Geological map of Tasikmalaya (Budhitrisna, 1990).

rock's physical properties and results in surface gravity difference. When gravity is measured, gravity acceleration g, g is proportional to mass m, where m is the outcome from density times volume. Hence measured gravity reflects the density and volume of subsurface rocks. The fundamental equation for the gravity method based on the law of Newton (1642–1727) is shown in Equation 1

$$\vec{F}\left(\vec{r}-\vec{r}_0\right) = -G\frac{m\cdot m_0}{\left|\vec{r}-\vec{r}_0\right|}\frac{\left(\vec{r}-\vec{r}_0\right)}{\left|\vec{r}-\vec{r}_0\right|} \qquad (1)$$

where, F is gravity force, G is gravity constant, m and m_0 are mass, and $r - r_0$ is the distance between 2 objects (Lowrie, 2007).

3.1 Derivative analysis

Derivative analysis was used for fault determination. The First Horizontal Derivative method (FHD) is used to determine the position and the Second Vertical Derivative (SVD) method for determining fault type. First Horizontal Derivative is the value of gravity anomaly changing horizontally. The changing anomaly at body contact has a sharp characteristic in the form of the maximum value of FHD (Blakely, 1995). So that it can be applied to indicate a geology structure border based on gravity anomaly, the peak point (maximum point) from the FHD curve could be associated with the fault or subsurface geology structure border. The second Vertical Derivative method is used for determining fault type based on the value of the SVD calculation. The value determines whether the fault is normal or reversed (Jacoby & Smilde, 2009). SVD acts as a high-pass filter, and the equation is derived directly from the Laplace equation for surface gravity anomaly (Jacoby & Smilde, 2009).

3.2 3D modelling

The purpose of 3D modeling was to characterize subsurface geological conditions based on density values. The method used was 3D inversion based on Pirttijarvi (2008). The iterative calculation is needed to obtain the optimum model matching the data observation. Softwares used for gravity 3D modeling were Grablox & Bloxer (Pirttijarvi, 2008). The Grablox program combines 2 inversion methods for calculation. The inversion methods

were Singular Value Decomposition and Occam inversion.

4 RESULTS AND DISCUSSION

The results from gravity data processing were 3 maps. The maps were the Complete Bouger Anomaly map (Figure 3), Regional Anomaly map (Figure 4), and Residual Anomaly map (Figure 5). The complete Bouger Anomaly (CBA) map resulted from gravity data processes from satellite data until gravity anomaly was obtained through several data corrections. From the CBA map, high anomaly values can be seen in the high terrain of the Galunggung area marked with purple to red color and making a closure pattern. This indicated a high-density contrast in the subsurface, possibly a heat source. High anomaly values can also be found in the southern part of the map. The high anomaly values are interpreted as derived from lithologies, such as limestone and plutonic intrusion. This interpretation is supported by the geology map of the Tasikmalaya sheet from Figure 2.

The Regional anomaly map resulted from the CBA map values being filtered with an upward continuation filter and only showing the regional anomaly. The regional anomaly was also defined as a low-frequency anomaly in the deeper position from the surface. From the regional anomaly map, high anomaly values can also be seen in the high terrain area of the Galunggung volcano. These high anomaly values are interpreted as heat sources and estimated as connected with the Karaha-Cakrabuana concession area at a deeper elevation. The residual anomaly map resulted from the CBA values subtracted with the regional anomaly values and called residual.

This residual map was used in interpreting shallow geothermal system components and usually affects a fairly small area. Permeable structures on the residual map are interpreted in areas with low anomaly values, namely dark blue ones, forming an elongated anomaly pattern, the presence of geothermal manifestations, and coinciding with the estimated fault position from the geology map of Tasikmalaya sheet (Budhitrisna, 1990), as well as the existence of the river. The authors interpreted three existing faults in the study area based on the earlier parameters. Further analysis was needed to interpret the structure thoroughly, so derivative analysis was conducted.

4.1 Derivative analysis

The results from the derivative analysis were 2 maps and several graphs. First Horizontal Derivative and Second Vertical Derivative maps (Figure 6). These 2 maps were derived from derivative analysis done on a regional map. Figure 6 shows the results of the structural interpretation in the study area, estimated from the results of the first horizontal derivative (FHD) and second vertical derivative (SVD) processing.

Interpretation is based on the maximum value on the FHD map marked in red to purplish red. Interpretation is also carried out by looking at the results of SVD processing. The drawing of the estimated structure line is based on looking at the zero value on the SVD map and the maximum value on the FHD map. If there was only zero value on the SVD map, but on the FHD map, there was no maximum value, then there was no structural response in that area. The interpretation of the two maps can only estimate the position of the existing structures in the study area. Analysis of SVD and FHD charts is required to estimate the presence of a permeable structure.

SVD analysis was used to estimate the type of structure in the study area. This analysis was in the form of a graphic profile of the incision results on a regional anomaly map which was then calculated until the SVD and FHD values were obtained. One of the results of the incision is shown in Figure 7. From this profile, it can be seen that the maximum value of the FHD graph coincides with the zero value on the SVD graph; this indicates the existence of a fault. Then from the calculation results, the value of |SVD| min, which is 0.000104 mGal/m^2, is smaller than the value of |SVD| max, which is 0.000194 mGal/m^2, so the existing fault is interpreted as a normal fault. Other incision profiles also supported this. Four of the six incision profiles showed the same result: normal fracture. This result means it supported the alleged fault from the Tasikmalaya sheet's geology map, which interprets the area as a normal fault, as seen in Figure 2.

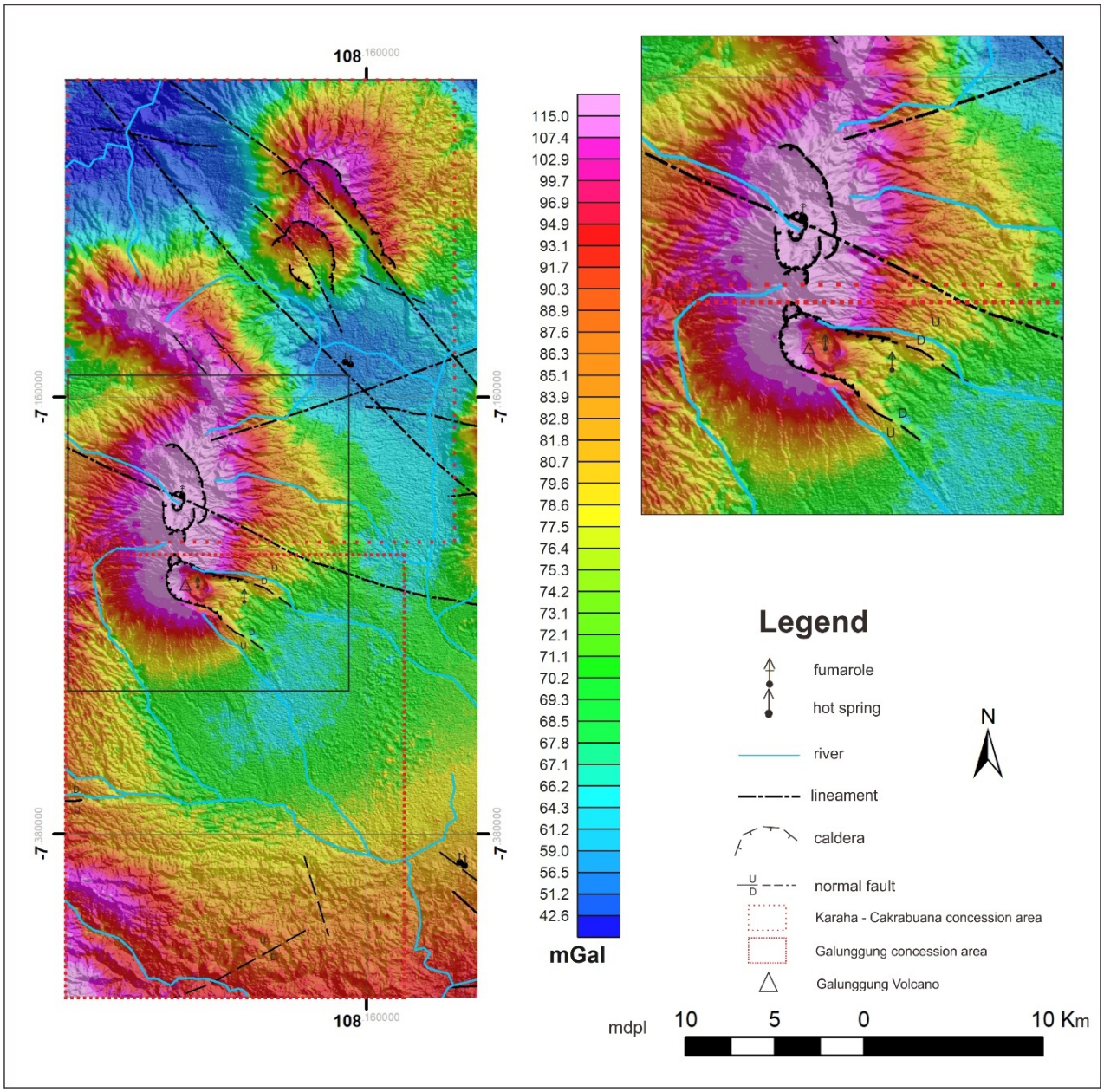

FIGURE 3. Complete Bouger anomaly map. Orange to purple color shows high anomaly values dominating around Galunggung Volcano and in the south of the map, interpreted as the young volcanic product. Yellow to blue shows low anomaly values dominating low-elevation areas, interpreted as old volcanic products..

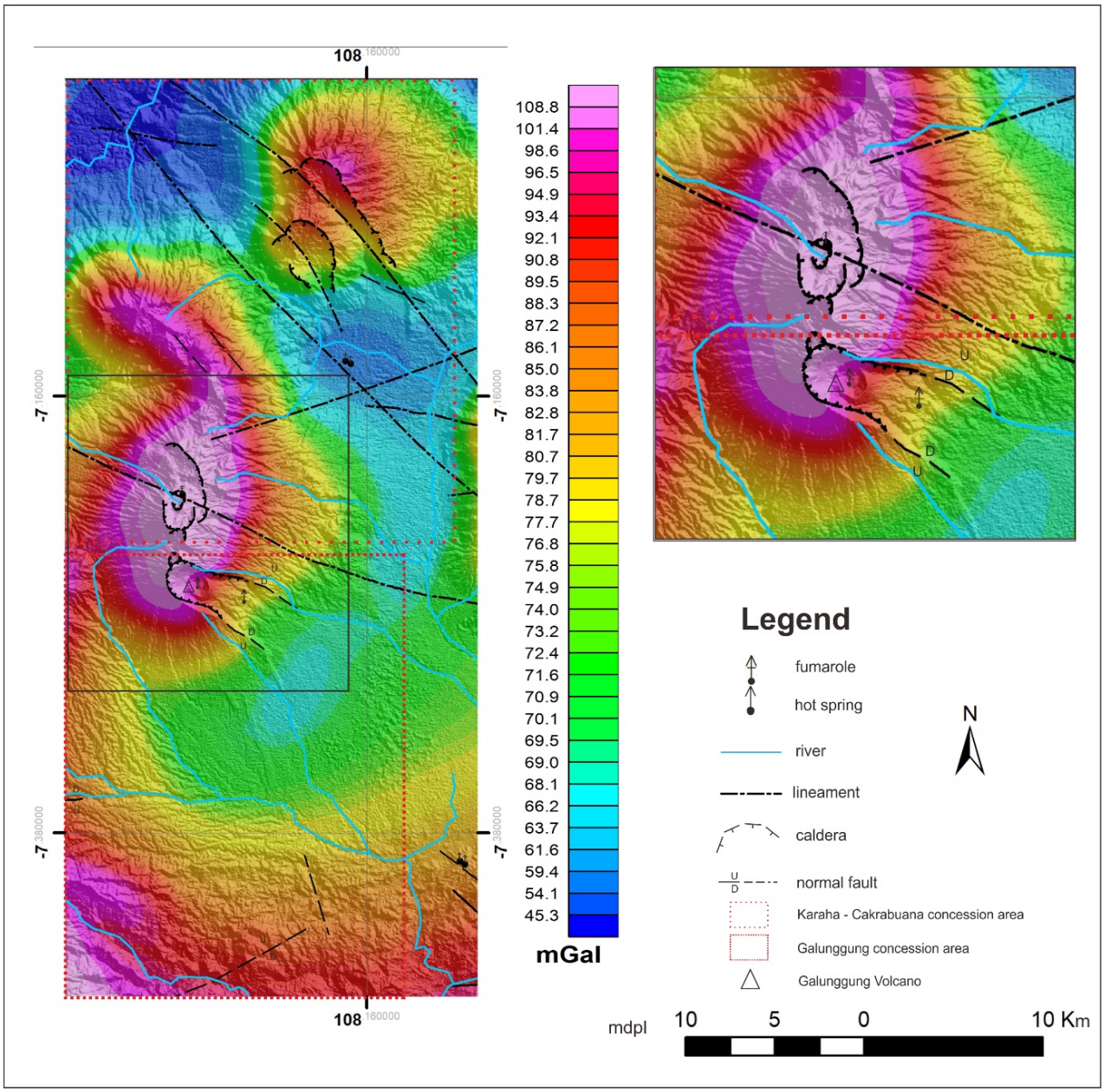

FIGURE 4. Regional anomaly map by using Upward Continuation Filter. Showing smoother contour lines in comparison with the CBA map..

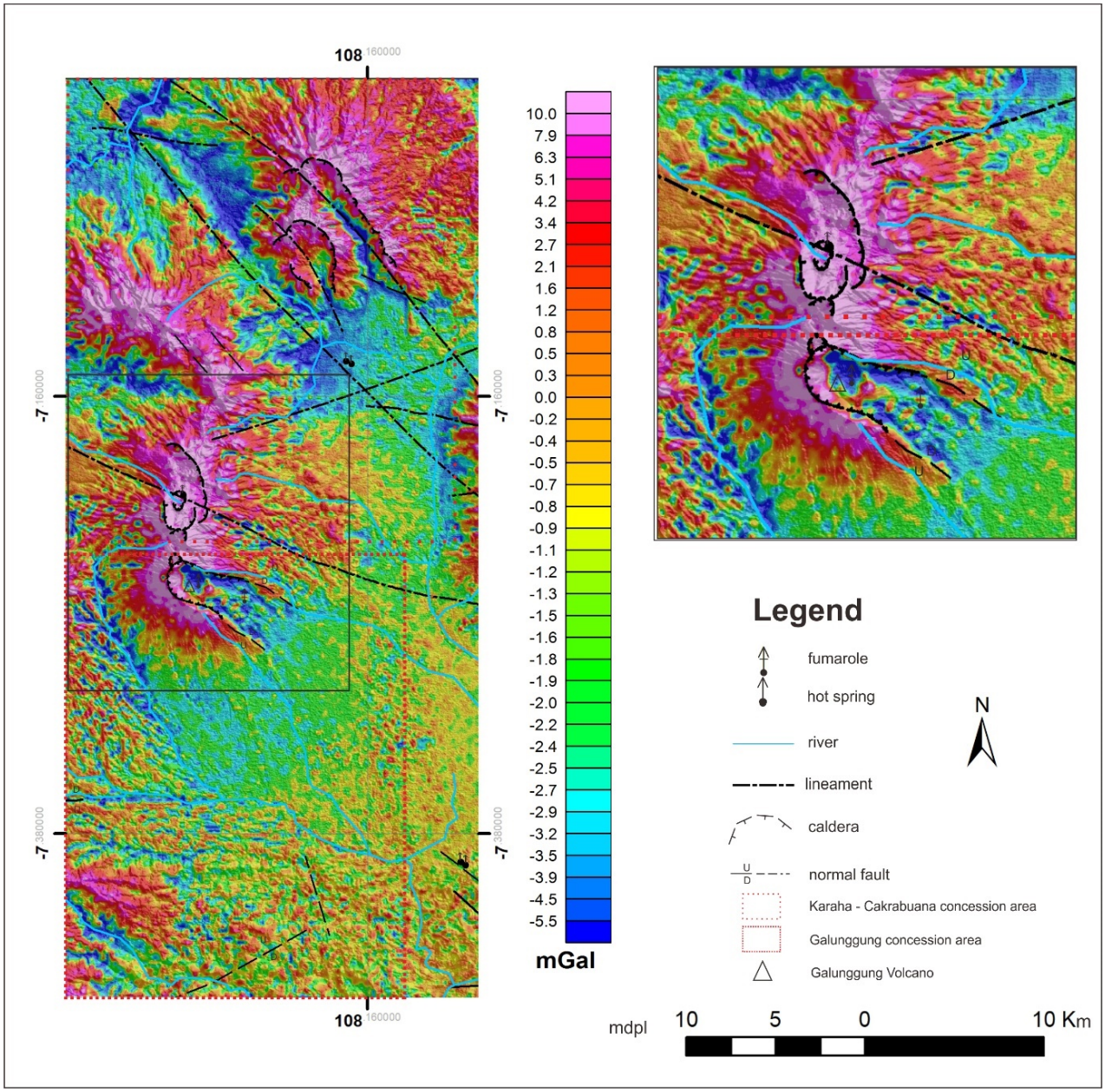

FIGURE 5. Residual anomaly map. High anomaly values (red to purple color) dominate in Galunggung and Karaha-Cakrabuana area and are interpreted as a response to andesitic rock. Low anomaly values (yellow to blue color) dominate in low-elevation areas around Galunggung and Karaha-Cakrabuana and are interpreted as tuff and breccia.

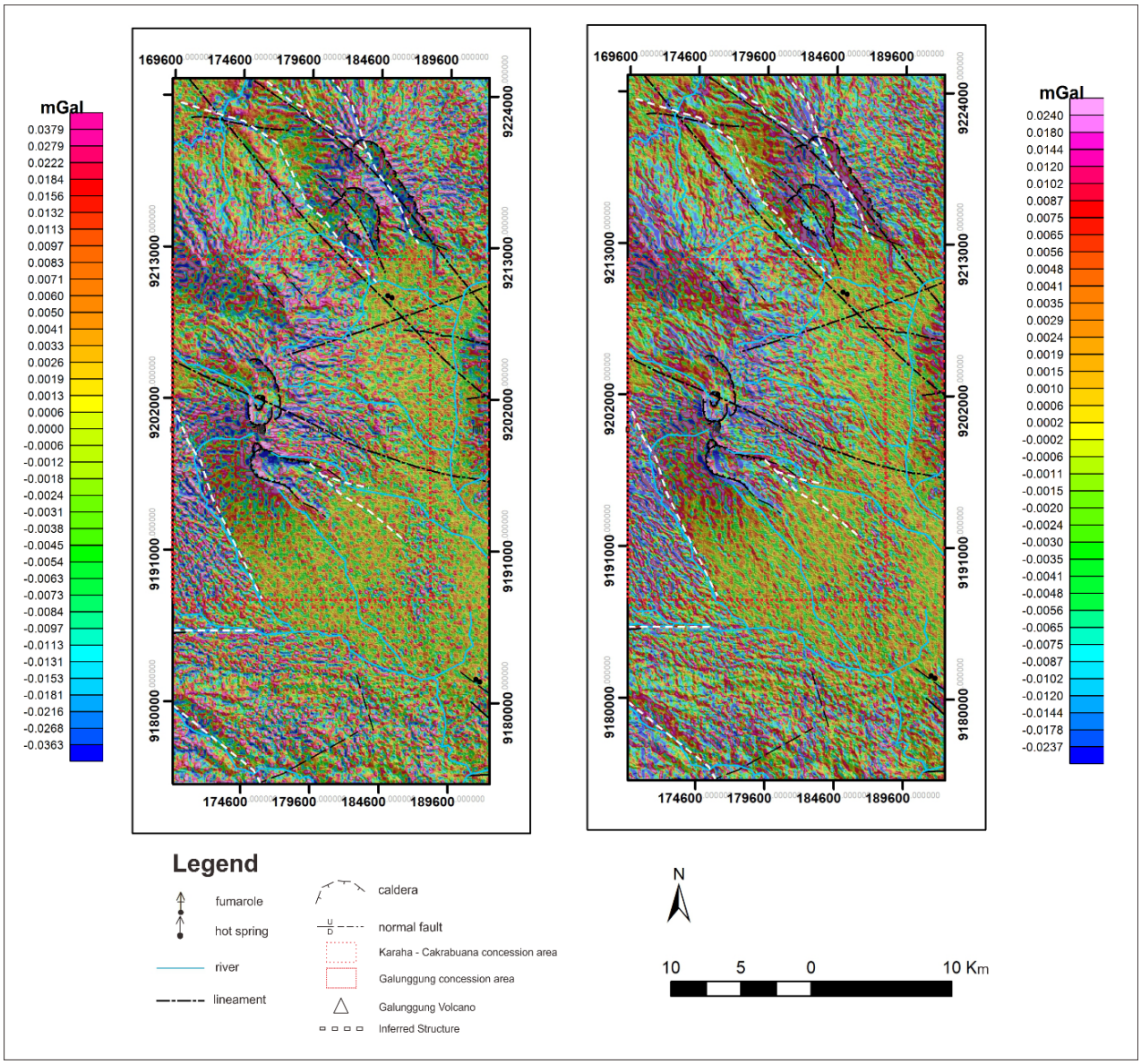

FIGURE 6. Interpretation of geological structures from Second Vertical Derivative map (Left) and First Horizontal Derivative map (right). White-colored dashed line acted as an interpreted fault position in the area; further analysis was needed to determine the fault type.

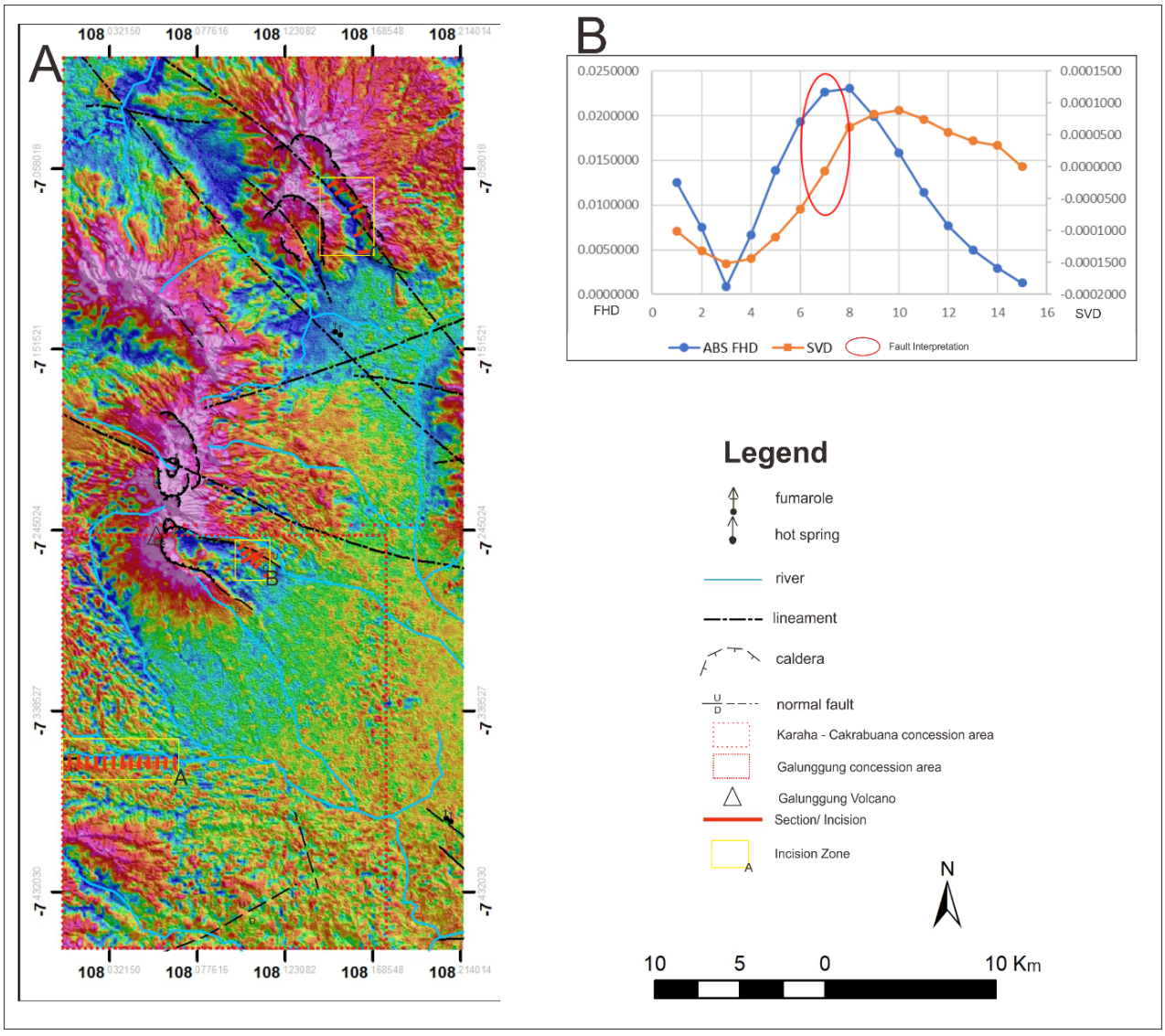

FIGURE 7. A) Regional anomaly map showing the location of the incision zone (marked with a yellow box). B) graph showing one of FHD vs SVD analysis in zone B. The red circle indicates the interpretation of normal fault.

4.2 3D model

The result from the 3D modeling process was the 3D model of the study area (Figure 8), sections A–A' (Figure 9), sections B–B' (Figure 10), and the conceptual model of the Galunggung geothermal area (Figure 11). Creating a 3D model starts with picking up the base map for the inversion process and, in this case, the regional map. After that, parameters must be set to ensure robust modeling. Lastly, an inversion process was carried out to obtain the 3D modeling. As shown in Figure 8, the result has 8.38 RMS (Root Mean Square) data error and 2.12% of model error. The density variation of the 3D model varied from 1.90 to 3.00 g/cm^3. To interpret the heat source of the 3D modeling results, as shown in Figure 8, was still quite difficult to do because the model was still a 3D model as a whole. Therefore, it was necessary to make an incision on the 3D model. The incisions made were trending north-south and in places that were the focus of the research, namely in the area near the summit of the Galunggung volcano. This incision was along the Y-axis coordinates, as shown in Figure 9. As can be seen in Figure 9, the position of the incision was shown on the 3d model with the point of view of the eagle eye and marked with black dots. The backward modeling graph along the sections was also displayed with matching curves between the measured and computed data overlaps with an rms data error value of 0.0838% and an RMS model of 0.0212%. In addition, the incision position was displayed in the 3d model or in the major block to provide a 3D view of the incision position.

In the cross-section of the cut results, it can be seen that at elevations above 0 km sea level, the densities vary from 1.90 gr/cm^3 to 2.86 gr/cm^3, marked in blue to red. This incision passes through two areas that are the focus of the research, namely the Galunggung peak and the Telaga Bodas crater. The peak of Galunggung is marked with a black triangle. The density that appears around the peak of Galunggung has a blue-to-red contrast. The green to orange color on the edge of the Galunggung peak is interpreted as the caldera of Galunggung volcano, and the blue color in the center is interpreted as the collapse of andesite breccias products from Galunggung volcano, which has been shown on the Tasikmalaya Geological map (Budhitrisna, 1990). In addition, the orange-to-red density beneath the Galunggung peak is thought to be a source of heat. Although the orange-to-red density extends over the entire section, the heat source from the Galunggung mountain was limited along the black dotted line only, and the one extending to the entire section is thought to be fresh intrusion rock.

Because of the software and computer restrictions, another 3D model was created for geothermal interpretation, and only the incision was shown. The incision was section B-B' as can be seen in Figure 10. This section then acted as a base for making the conceptual model of the Galunggung geothermal area (Figure 11). The conceptual model was also made by inferring from various sources (Henley & Ellis, 1983; Tripp et al., 2002; Reynolds, 2011; Yosephin et al., 2019). The estimated reservoir boundary and cap rock were interpreted from the B–B' cut profile. The cap rock was estimated to be at the top of Galunggung volcano and up to a depth of 0 masl, which was seen from the density contrast in blue with a value of less than 2.3 gr/cm^3 and was thought to be a tuff whose rock porosity has been filled with altered minerals. The geothermal reservoir of the Galunggung CA was estimated to have a density of around 2.3–2.6 gr/cm^3 which was indicated by a green density contrast. The Galunggung reservoir's upper limit was 0–2 km above sea level, marked with a dotted line in Figure 11. The reservoir rock of the Galunggung geothermal system was interpreted as a volcanic breccia that has developed due to normal fault activity near the Galunggung crater. The volcanic breccia has a density value of about 2.3–2.6 gr/cm^3. For a 2.6–2.8 gr/cm^3 density, it was interpreted as andesite rock extending from the Galunggung volcano to the southern part of the Galunggung volcano. The andesite rock is thought to be a hot rock that is a source of heat in the Galunggung volcano area. However, the heat source of the Galunggung geothermal system was estimated to have a density of more than 2.8 gr/cm^3 with a density contrast in red and its location below the summit of the Galunggung volcano.

The heat source was estimated to be be-

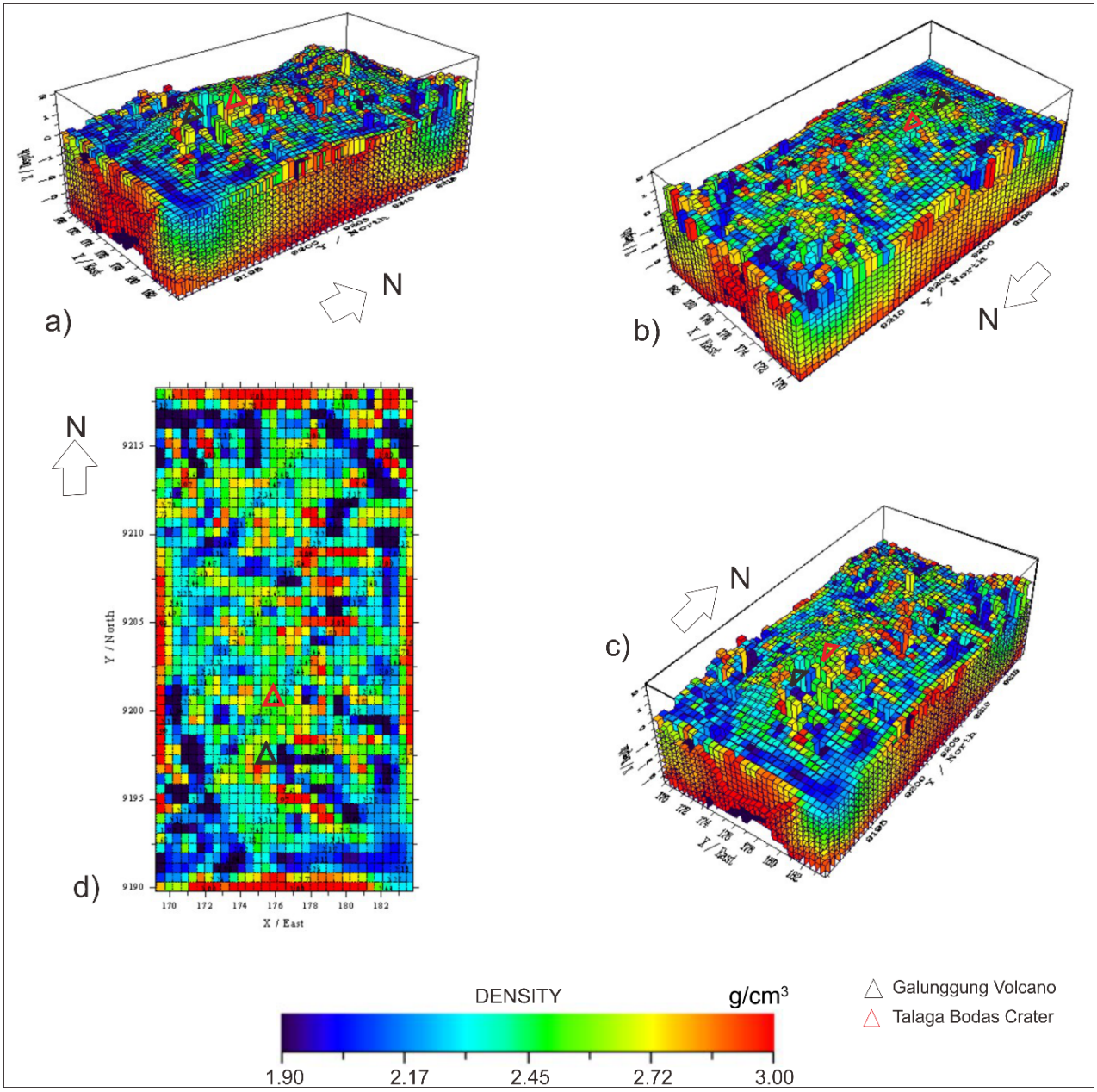

FIGURE 8. 3D Model from Grablox 1.6e shows the study area's density variation.

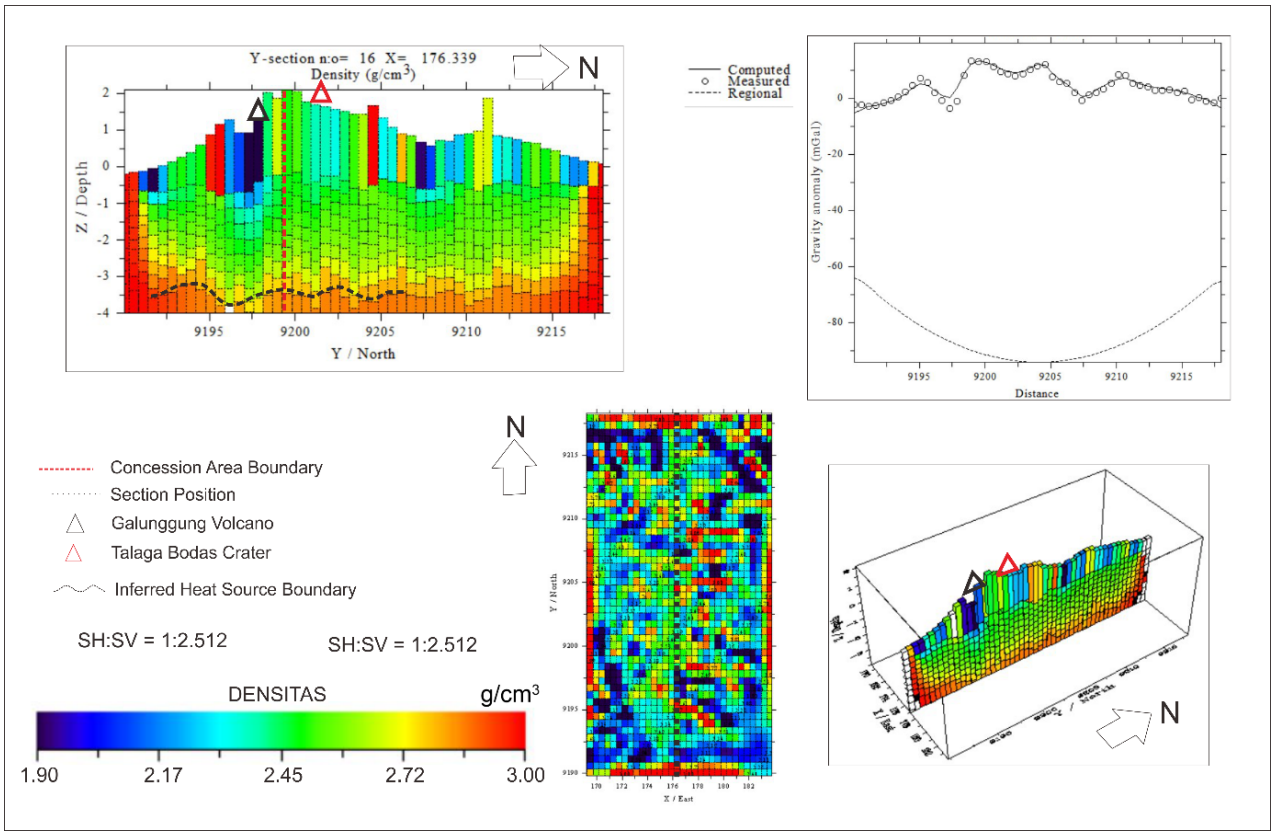

FIGURE 9. Section A–A′.

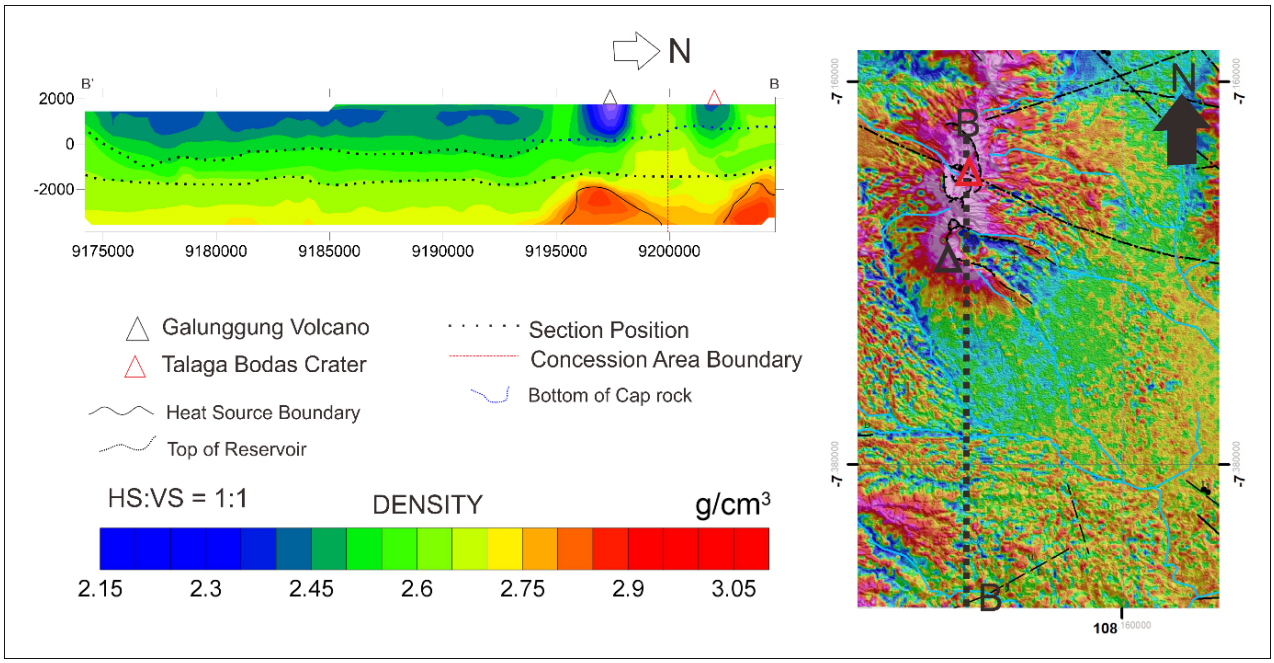

FIGURE 10. Section B–B′.

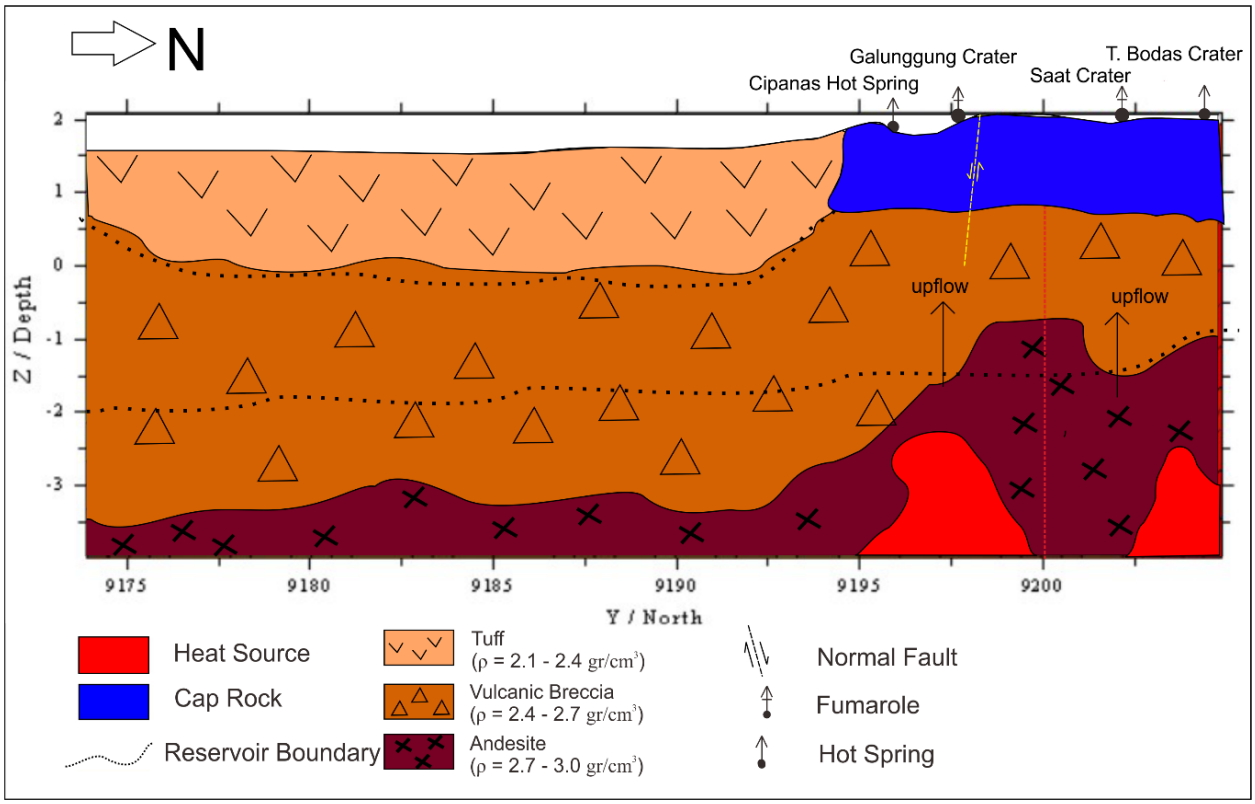

FIGURE 11. Conceptual model of Galunggung geothermal area.

low 2 km above sea level, with the center of the intrusion just below the Galunggung crater marked by red contrast. The interpretation of heat sources was supported by the presence of geothermal manifestations in the form of fumaroles and hot springs (acting as an upflow) in the crater of the Galunggung volcano (Bronto, 1989). The heat source is estimated to be andesite, with a density between 2.8 gr/cm^3 to 3.0 gr/cm^3. The reservoir zone marked in green was near the intrusion center. The cap of the Galunggung CA geothermal system is thought to be a tuff that interacts with the condensate layer (formed above the reservoir zone), and then the minerals alter and fill the rock porosities to form an impermeable layer. A black dashed line marked the estimated boundary between the cap and the reservoir zone.

The reservoir zone was considered a volcanic breccia rock, a product of the Galunggung mountain, caused by intrusions and normal faults on the summit of the Galunggung volcano. These faults were supported by analysis of the FHD and SVD derivatives of the zone B section (Figure 6), which showed a normal fracture response. The normal fault was considered a permeable structure that leads to an exit from the upflow zone of the Galunggung geothermal system. This was supported by the Cipanas hot spring's appearance near the Galunggung volcano's summit. From the response to the gravity data in the concession area of Galunggung volcano, it was estimated that the developing geothermal system was similar to the geothermal system of the Karaha-Cakrabuana WKP, considering its location adjacent to the Karaha-Cakrabuana WKP. In addition, the two concession area heat sources might have been connected at depths below 2 km above sea level, as shown in section A–A' (Figure 9).

5 CONCLUSION

The gravity anomaly pattern that showed the presence of a fault was an anomaly pattern that forms an alignment and has a contrast value that changes quite drastically from low to high or vice versa, as seen in the residual map. While for heat sources, the anomaly pattern was indicated as a gravity anomaly that forms a closure pattern and is marked with a high value, as seen on the CBA map, residual and regional maps. The continuity pattern of the permeable struc-

ture in the study area was characterized by the presence of a zero value on the SVD value that coincides with the maximum FHD value and is supported by a continuous anomaly pattern from low to high values. From the analysis results, the existing faults in the study area were normal.

REFERENCES

Blakely, R. J. (1995). *Potential Theory in Gravity and Magnetic Applications.* New York: Cambridge University Press. 441 pages.

Bronto, S. (1989). *Volcanic Geology of Galunggung, West Java, Indonesia.* [Unpublished doctoral dissertation]. University of Canterbury, Canterbury, 343 pages.

Budhitrisna, T. (1990). *Peta Geologi Lembar Tasikmalaya.* Pusat Penelitian dan Pengembangan Geologi, Bandung, Jawa Barat, Indonesia

Fadillah, A., Nugraha, T., & Gumilar, J. (2013). *West Java Geothermal Update* [Paper presentation]. Thirty-Eighth Workshop on Geothermal Reservoir Engineering, Stanford University, California.

Hall, R. (2002). Cenozoic geological and plate tectonic evolution of SE Asia and the SW Pacific: Computer-based reconstructions, model and animations. *Journal of Asian Earth Sciences*, 353-431.

Henley, R., & Ellis, A. (1983). Geothermal Systems, Ancient and Modern: A Geochemical Review. *Earth Science Reviews*, 19, 1–50.

Hirt, C., Claessens, S., Fecher, T., Kuhn, M., Pail, R., & Rexer, M. (2013). New ultra-high resolution picture of Earth's gravity field. *Geophysical Research Letters*, 40, 24 pages.

Jacoby, W., & Smilde, P.L. (2009) *Gravity Interpretation: Fundamentals and Application of Gravity Inversion and Geological Interpretation*. Springer-Verlag, Berlin, 395p.

Kementerian Energi dan Sumberdaya Mineral RI (2017) *Potensi Panas Bumi Indonesia Jilid 1.* Direktorat Panas Bumi, Direktorat Jenderal Energi Baru, Terbarukan dan Konservasi Energi Kementerian Energi dan Sumberdaya Mineral, Jakarta. 803p.

Lowrie, W. (2007). *Fundamentals of Geophysics.* Cambridge: Cambridge University Press. 362p.

Pirttijarvi, M. (2008). *Grablox, Gravity Interpretation and Modelling Software Based on a 3-D Block Model, User's Guide*. University of Oulu Press, Oulu, 31p.

Pulunggono, A., & Martodjojo, S. (1994). *Perubahan Tektonik Paleogen dan Neogen merupakan peristiwa terpenting di Jawa* [Paper presentation, in Bahasa]. Prosiding Geologi dan Geoteknik Pulau Jawa sejak Akhir Mesozoic hingga Kuarter, Yogyakarta, page 37-50.

Ramadhan, Q., Sianipar, J., & Pratopo, A. (2016). *Volcanostratigraphic Approach for Evaluation of Geothermal Potential in Galunggung Volcano*. The 5th ITB International Geothermal Workshop, 8 pages.

Reynolds, J.M. (2011). *An Introduction to Applied and Environmental Geophysics.* 2nd Edition. John Wiley & Sons, Ltd., Oxford, 696p.

Tripp, A., Moore, J., Ussher, G., & McCulloch, J. (2002). *Gravity Modelling of The Karaha-Telaga Bodas Geothermal System* [Paper presentation]. Proceedings of the Twenty-seventh Workshop on Geothermal Reservoir Engineering, Stanford University Press, Stanford, pages 28-30.

Van Bemmelen, R. (1949). *The Geology of Indonesia.* Volume 1. Government Printing Office, The Hague, Netherlands, 766p.

Yosephin, M., Santoso, D., & Setianingsih. (2019). The Subsurface Modelling of Karaha-Telaga Bodas Geothermal System using Gravity Method. *IOP Conf. Ser.: Earth Environ. Sci.* 318 012037. https://doi.org/10.1088/1755-1315/318/1/012037.